


# Adipose-Derived Mesenchymal Stromal/ Stem Cell Line Prevents Hepatic Ischemia/Reperfusion Injury in Rats by Inhibiting Inflammasome Activation

Cell Transplantation  
Volume 31: 1–15  
© The Author(s) 2022  
Article reuse guidelines:  
sagepub.com/journals-permissions  
DOI: 10.1177/09636897221089629  
journals.sagepub.com/home/cll  


Kaili Chen<sup>1</sup>, Hideaki Obara<sup>1</sup> , Yumiko Matsubara<sup>2</sup>,  
Kazumasa Fukuda<sup>1</sup>, Hiroshi Yagi<sup>1</sup>, Yukako Ono-Uruga<sup>2</sup>,  
Kentaro Matsubara<sup>1</sup>, and Yuko Kitagawa<sup>1</sup>

## Abstract

Mesenchymal stromal/stem cells (MSCs) have shown potential in the treatment of degenerative diseases, including ischemia/reperfusion injury (IRI), which occurs during organ transplantation and represents the main cause of post-transplant graft dysfunction. However, MSCs have heterogeneous characteristics, and studies of MSCs therapy have shown a variety of outcomes. To establish a new effective MSCs therapy, we developed an adipose-derived mesenchymal stromal/stem cell line (ASCL) and compared its therapeutic effects on primary adipose-derived MSCs (ASCs) using a hepatocyte co-culture model of hypoxia/reoxygenation *in vitro* and a rat model of hepatic IRI *in vivo*. The results showed that both ASCL and ASCs protect against hypoxia by improving hepatocyte viability, inhibiting reactive oxygen species release, and upregulating transforming growth factor- $\beta$  *in vitro*. *In vivo*, ASCL or ASCs were infused into the spleen 24 h before the induction of rat hepatic IRI. The results showed that ASCL significantly improved the survival outcomes compared with the control (normal saline infusion) with the significantly decreased serum levels of liver enzymes and less damage to liver tissues compared with ASCs. Both ASCL and ASCs suppressed NOD-like receptor family pyrin domain-containing 3 inflammasome activation and subsequently reduced the release of activated IL-1 $\beta$  and IL-18, which is considered an important mechanism underlying ASCL and ASCs infusion in hepatic IRI. In addition, ASCL can promote the release of interleukin-1 receptor antagonist, which was previously reported as a key factor in hampering the inflammatory cascade during hepatic IRI. Our results suggest ASCL as a new candidate for hepatic IRI treatment due to its relatively homogeneous characteristics.

## Keywords

liver transplantation, cell therapy, hepatic ischemia/reperfusion injury, inflammasome, mesenchymal stem cells

## Introduction

Hepatic ischemia/reperfusion injury (IRI) occurs when the blood supply is temporarily interrupted and restored to perfuse into the liver tissue during liver transplantation or hepatic lesions of surgical origin. It is one of the most severe postoperative complications, causing liver dysfunction and complex multiple organ failures. The induction of reactive oxygen species (ROS) and inflammatory response by ischemia and reperfusion are the primary causes of hepatic injury<sup>1,2</sup>. At the early stage of hepatic IRI, ROS released by the activation of Kupffer cells and endothelial cells induces direct cellular injury<sup>3</sup>. Proinflammatory cytokines and chemokines are subsequently triggered in the intermediate stage of hepatic IRI by oxidative stress<sup>4</sup>. Cytokines such as tumor necrosis factor- $\alpha$  (TNF- $\alpha$ ), interleukin (IL)-1, IL-6, and

IL-18, which are generated mainly from leukocytes, promote inflammation in liver tissue and eventually induce cell death in hepatocytes at the late stage of hepatic IRI<sup>5</sup>.

Mesenchymal stromal/stem cells (MSCs) are a type of multipotent cells capable of self-renewal and differentiation

<sup>1</sup> Department of Surgery, Keio University School of Medicine, Tokyo, Japan

<sup>2</sup> Clinical and Translational Research Center, Keio University School of Medicine, Tokyo, Japan

Submitted: January 24, 2022. Revised: March 2, 2022. Accepted: March 5, 2022.

### Corresponding Author:

Hideaki Obara, Department of Surgery, Keio University School of Medicine, 35 Shinanomachi, Shinjuku-ku, Tokyo 160-8582, Japan.  
Email: obara.z3@keio.jp



into multiple somatic cells such as adipocytes, osteoblasts, and chondroblasts<sup>6</sup>. MSCs have been reported to be effective in treating various degenerative diseases, including liver diseases<sup>7–11</sup>. Compared with other types of stem cell therapies, such as induced pluripotent stem cells and embryonic stem cells, MSCs therapy has the advantage of easy access and presents no concern regarding ethical problems and immune tolerance<sup>12</sup>. Therefore, MSCs transplantation is a potential candidate for alleviating hepatic IRI. Several preclinical studies have shown that MSCs transplantation improves liver function, promotes hepatocyte proliferation, and suppresses hepatic degeneration in the animal liver injury models<sup>13–19</sup>, in which the paracrine of soluble factors such as transforming growth factor- $\beta$  (TGF- $\beta$ ) and IL-10 is potential therapeutic effects of MSC transplantation<sup>15,20,21</sup>. However, because MSCs are heterogeneous<sup>6</sup>, clinical trials of MSCs therapy for liver diseases have shown a variety of different outcomes<sup>22–25</sup>. In a randomized controlled trial, administration of autologous bone marrow MSCs (BMSCs) in alcoholic cirrhosis patients improved their liver functions and Child-Pugh scores<sup>25</sup>. However, Mohamadnejad et al.<sup>23</sup> revealed an opposite result, as no significant improvement of Child score, model for end-stage liver disease score, or liver function was found in their randomized controlled trial of autologous BMSCs treatment of liver cirrhosis. Although no clinical trials of MSCs therapy in hepatic IRI were published so far (end of December 2021), a phase I–II clinical trial showed that MSCs treatment after liver transplantation did not improve the overall rates of rejection or graft survival<sup>22</sup>, suggesting that this therapy requires further improvement before its practical use in hepatic IRI treatment.

In a previous study, we established a human adipose-derived mesenchymal stem/stromal cell line (ASCL) purified from traditional adipose-derived MSCs (ASCs) and fulfilling the common definition of MSCs<sup>26</sup>. In the process of platelet-like cell generation from both ASCs and ASCL, the latter is superior to ASCs in terms of stability and efficiency when differentiating into megakaryocytes, suggesting that ASCL is more homogeneous and has greater differentiation ability than ASCs<sup>26</sup>. In the present study, we aimed to investigate the effect of ASCL in the animal hepatic IRI model on whether it has any progress in therapeutic potential in comparison with autologous ASCs. We focused on the immune response related to hepatic IRI, and ASCL was observed to suppress the NOD-like receptor family pyrin domain-containing 3 (NLRP3) inflammasome activation and to upregulate IL-1 receptor antagonist (IL-1Ra). As a result, we consider ASCL as a new candidate for hepatic IRI treatment.

## Materials and Methods

### *Animals and Ethical Considerations*

Male Wistar rats aged 7 weeks and weighing 200–250 g were obtained from the Sankyo Labo Service Corporation (Tokyo, Japan). All animal experiments were carried out in

accordance with the National Institutes of Health Guide for the Care and Use of Laboratory Animals (NIH Publication No.8023, revised 1978). All experimental procedures were approved by the Ethics Committee of Keio University and the Laboratory Animal Center, Keio University School of Medicine (approval number: 20018).

### *Extraction and Cell Culture of ASCL and ASCs*

The extraction of ASCL and ASCs was performed as previously described<sup>26</sup>. Briefly, subcutaneous adipose tissue obtained from Wistar rats under isoflurane anesthesia (Pfizer Inc., New York, NY, USA) was minced and digested with collagenase IV (Sigma-Aldrich, Burlington, MA, USA). The digested adipose suspension was then filtered through a 70- $\mu$ m mesh and centrifuged at 1200 rpm for 5 min to obtain the stromal vascular fraction pellet, which was resuspended in high-glucose Dulbecco's modified Eagle's medium (DMEM; Nacalai, Tokyo, Japan) supplemented with 20% fetal bovine serum (FBS) and 100 U/mL penicillin-streptomycin (P-S). After incubation in a 100-mm Petri dish, adhered cells were considered ASCs, and therefore selected by exchanging the culture media 24 h after seeding.

ASCL was obtained from pre-existing ASCs. ASCs, at the third passage, were differentiated into adipocytes in T-75 flasks using rat adipocyte differentiation medium (Cell Applications Inc., San Diego, CA, USA). Cell cultures were gently washed twice with phosphate buffered salts (PBS) and trypsinized mildly with two additional PBS washing after 2 weeks of differentiation. Fat-drop from the trypsinized and centrifuged cells underwent an upside-down culture. The flasks were then fully filled with high-glucose DMEM supplemented with 20% FBS and 100 U/mL P-S. Fat-drop from trypsinized adipocytes was floated and attached to the ceiling of flasks due to their low density, once the dedifferentiation was completed after 2 weeks without medium change. The flasks were inverted and cultured with medium change using the same condition to ASCs described above.

### *Osteoblasts and Adipocytes Differentiations of ASCL and ASCs*

ASCs were differentiated into osteoblasts in osteogenic differentiation medium (PromoCell, Heidelberg, Germany). Alkaline phosphatase of differentiated cells was visualized using the BCIP-NBT Solution Kit for Alkaline Phosphatase Stain (Nacalai), and differentiated into mature adipocytes in adipocyte differentiation medium (Cell Applications Inc.). Lipid accumulation in adipocytes was visualized by Oil Red O (Nacalai) according to the manufacturer's protocol.

### *Phenotyping and RNA-Sequencing of ASCL and ASCs*

For flow cytometry and RNA-sequencing analysis, ASCL and ASCs were harvested in three passages. CD44-FITC

(BioLegend, San Diego, CA, USA), CD90-APC (BioLegend), CD34 (Santa Cruz Biotechnology, Dallas, TX, USA), and CD45-PE (BioLegend) were detected by BD FACS flow cytometry (BD, Franklin Lakes, NJ, USA).

For RNA-sequencing, total RNA obtained from each sample was subjected to a sequencing library construction using the SureSelect Strand Specific RNA Library Preparation Kit for Illumina (Agilent Technologies Inc., Santa Clara, CA, USA) according to the manufacturer's protocol. The quality of the libraries was assessed using an Agilent 2200 TapeStation D1000/High Sensitivity (Agilent Technologies). The pooled libraries of the samples were sequenced using the HiSeq system (Illumina Inc., San Diego, CA, USA) in 51-base-pair single-end reads.

For functional enrichment analysis, all differentially expressed genes (DEGs) of ASCL and ASCs were determined via  $|\log_2 \text{fold change}|$  and mapped to terms in the gene ontology (GO) database (<http://geneontology.org>). Significantly enriched GO terms were searched for among the DEGs considering  $P < 0.05$ .

### Rat Hepatocytes Isolation

For hepatocyte isolation, Wistar rats were anesthetized with isoflurane (Pfizer Inc.). The portal vein was cannulated with an 18-gauge catheter and perfused in 150 mL of Hanks' balanced salt solution supplemented with collagenase IV (Sigma-Aldrich). The vena cava was immediately cut to flush the perfusion fluid. Hepatocytes were dispersed in the digested liver tissue by manual shaking and then filtered through a 100-mm mesh. Isolated hepatocytes were subjected to Percoll density-gradient centrifugation (GE Healthcare, Marlborough, MA, USA). The final hepatocyte viability was determined by trypan blue staining. Cells were seeded in collagen-coated 6-well plates at  $5 \times 10^5$  cells/well and cultured in high-glucose DMEM supplemented with 10% FBS, 100 U/mL P-S, 25  $\mu\text{g/mL}$  epidermal growth factor, 2 U/mL GlutaMAX, 1  $\mu\text{M}$  dexamethasone, and 1% insulin-transferrin serum at 37°C in a 5% CO<sub>2</sub> humidified atmosphere.

### Cell Co-culture and Hypoxia/Reoxygenation Conditioning Culture

Hepatocyte culture with ASCs or ASCL was performed 6 h after the attachment of isolated hepatocytes. ASCs or ASCL were seeded at a density of  $1 \times 10^5$  cells/well. Single cultures were used as the control group. After 24 h of co-culture, both groups were transferred to no-glucose DMEM (Nacalai) and incubated under hypoxic conditions in a modular incubator chamber with 1% O<sub>2</sub> and 5% CO<sub>2</sub> in a humidified atmosphere for 3 h. After this period, the culture medium of both groups was replaced with high-glucose DMEM plus supplements and samples were returned to the normal incubation environment for 1 h before being collected and frozen. Culture cells were harvested as frozen pellets or fixed in 4% paraformaldehyde for further analysis.

### Rat Hepatic IRI Model and Cell Therapy

Segmental (70%) hepatic warm ischemia was performed under isoflurane (Pfizer Inc.) anesthesia, as previously described<sup>27</sup>. Briefly, an aneurysm clip (Sugita, Tokyo, Japan) was used to clamp the bile duct, portal vein, and hepatic artery of the median and left lobes of the liver. After 60 min of ischemia, the clip was removed to re-perfuse the blood flow. Cell infusion of ASCs or ASCL was performed intrasplenic at  $1 \times 10^6$  cells/rat 24 h before hepatic IRI induction. Saline was injected intrasplenic in the control group. Rats were sacrificed at 3 and 24 h after reperfusion ( $n = 5$  for each group) and serum and injured liver tissue samples were collected for further analysis. We also performed segmental (70%) hepatic warm ischemia in each group for 120 min to induce lethal hepatic injuries and examined the 10-day survival ( $n = 10$  for control group,  $n = 6$  for ASCL and ASCs group).

### Liver Function Tests

Serum alanine aminotransferase (ALT) and serum aspartate aminotransferase (AST) levels were analyzed by SRL (Tokyo, Japan).

### Western Blotting and Enzyme-Linked Immunosorbent Assay (ELISA)

Western blotting was performed to analyze the expression of NLRP3 (ABclonal, Woburn, MA, USA), caspase-1 (casp-1; Sigma-Aldrich), IL-1 $\beta$  (Abcam, Cambridge, UK), IL-18 (R&D Systems, Minneapolis, MN, USA), IL-1RA (Abcam), and  $\beta$ -actin (Cell Signaling Technology, Danvers, MA, USA) in liver tissues according to the manufacturer's protocol. Serum concentrations of TGF- $\beta$  (R&D Systems), IL-6 (R&D systems), IL-10 (Thermo Fisher Scientific, Waltham, MA, USA), and IL-18 (Thermo Fisher Scientific) were detected using an ELISA kit according to the manufacturer's protocol.

### Cell Images and Histology Study

Paraformaldehyde-fixed cell cultures were stained for DNA fragmentation using the DeadEnd Fluorometric TUNEL System (Promega, Madison, WI, USA) and an anti-albumin antibody (Abcam). Hepatocytes were distinguished from ASCs/ASCL in the co-culture group as albumin-positive stained cells. ROS was detected in cell cultures using an ROS assay kit (Dojindo, Tokyo, Japan) according to the manufacturer's protocol.

The liver tissue of each group was fixed using 4% paraformaldehyde phosphate buffer solution at 4°C. The sections were cut to a thickness of 4  $\mu\text{m}$  and stained with hematoxylin and eosin for histological examination. The TUNEL assay was performed using the DeadEnd fluorometric TUNEL system (Promega).

**Table 1.** Gene-Specific Primers Used in the Quantitative Real-Time Polymerase Chain Reaction Assay in the Current Study.

Primer	Forward	Reverse
TGF- $\beta$ 1	5'-CGTTACCTTGGAACCGGCT-3'	5'-AGCCCTGTATTCCGTCCT-3'
IL-10	5'-GAAGGACCAGCTGGACAACA-3'	5'-TCAGCTTCTCTCCCA-3'
IL-1Ra	5'-CGCTTTACCTTCATCCGCTC-3'	5'-GGGCTCTTTGGTGTGTTGG-3'
IL-6	5'-AGAGACTTCCAGCCAGTTGC-3'	5'-TCTGACAGTGCATCATCGCT-3'
GAPDH	5'-GAAGGTCGGTGTGAACGGAT-3'	5'-ACCAGCTTCCCATTCTCAGC-3'

GAPDH: glyceraldehyde-3-phosphate dehydrogenase; IL: interleukin; TGF- $\beta$ 1: transforming growth factor- $\beta$ 1.

### Quantitative Real-Time Polymerase Chain Reaction (qRT-PCR)

Total RNA was extracted from co-cultured cells and liver tissue using the RNeasy Plus Mini Kit (QIAGEN, Hilden, Germany). For quantification of TGF- $\beta$ 1, IL-10, and IL-1Ra expression, total RNA was reverse transcribed into cDNA using a BIO-RAD iScript cDNA Synthesis Kit (Hercules, CA, USA). qRT-PCR was performed using the ViiA 7 RT-PCR system (Thermo Fisher Scientific). The primers used are listed in Table 1.

### Viability and Lactate Dehydrogenase (LDH) Assessment After Hypoxia/Reoxygenation Lesion

The viability of cell cultures was assessed using cell counting kit-8 (Dojindo), and LDH in conditioned media was measured using an LDH assay kit (Abcam) according to the manufacturer's protocol.

### Data Analysis

Values are expressed as mean  $\pm$  standard error (SE). The curves of survival rates were created using the Kaplan Meier method. The statistical significance of the differences between groups was evaluated using the log-rank test for the survival rates and Student's *t*-test for all the other data ( $P < 0.05$ ) using JMP 14 software (<https://www.jmp.com/>).

## Results

### Characterization of Rat ASCL and ASCs

Rat ASCL and ASCs were both analyzed by flow cytometry at passage 3 for the expression of cell surface molecules. Both were positive for CD44 and CD90 and negative for CD45 and CD34 expression (Fig. 1A).

In the differentiation capacity examination, both ASCL and ASCs were verified to differentiate into adipocytes or osteoblasts and successfully stained positive for Oil Red O and alkaline phosphatase staining, respectively (Fig. 1B).

To investigate the overall biological functions elicited by ASCLs and ASCs. Analyses of DEGs and GO terms identified a stronger enrichment for functions related to hypoxia and inflammatory response in ASCL than in

ASCs, specifically in the cellular response to IL-1 (Fig. 2, Supplemental Table 1).

### ASCL and ASCs Attenuate Hepatocytes Hypoxia/Reoxygenation Damage in Co-culture

To assess the cytoprotective effects of ASCL and ASCs against hepatocytes hypoxia/reoxygenation damage, rat ASCL and ASCs were co-cultured with rat hepatocytes. Hypoxia was applied to co-culture and single culture of hepatocytes (control) groups for 3 h and these were returned to normal incubation conditions for 1 h to stimulate reperfusion. All cells were evenly distributed after seeding in 6-well plates (Fig. 3A). Hepatocytes in the control group were abundantly detached from the bottom plate after the hypoxia/reoxygenation treatment, whereas the attachment of hepatocytes was maintained in the ASCs and ASCL co-culture groups (Fig. 3B). Cell apoptosis was analyzed by TUNEL cell staining (Fig. 3C). A decrease in hepatocyte cell death was observed in both ASCL ( $P < 0.001$ ) and ASCs ( $P < 0.001$ ) co-culture groups compared with the single hepatocytes culture group (Fig. 3D). Increased LDH levels in the culture medium were detected in the control group after the hypoxia/reoxygenation treatment, whereas it was suppressed in ASCs ( $P < 0.001$ ) and ASCL ( $P = 0.005$ ) co-cultures (Fig. 3E). Moreover, cell viability in the different groups was further assessed by the cell counting kit-8 (Fig. 3F), and statistical differences were found between the single and co-culture groups ( $P < 0.01$ ).

### ASCL and ASCs Protect Hepatocytes From ROS Damage

We detected ROS expression after the hypoxia/reoxygenation treatment by cell imaging intensity (Fig. 4A). ROS induction was significantly decreased in ASCs ( $P < 0.001$ ) and ASCL ( $p < 0.001$ ) co-culture groups compared with the control group (Fig. 4B).

### ASCL and ASCs Upregulate the Expression of Cytoprotective Cytokines Under Hypoxia

In the qRT-PCR study, we measured the mRNA expression of cytoprotective cytokines (TGF- $\beta$ , IL-10, and IL-1Ra) in



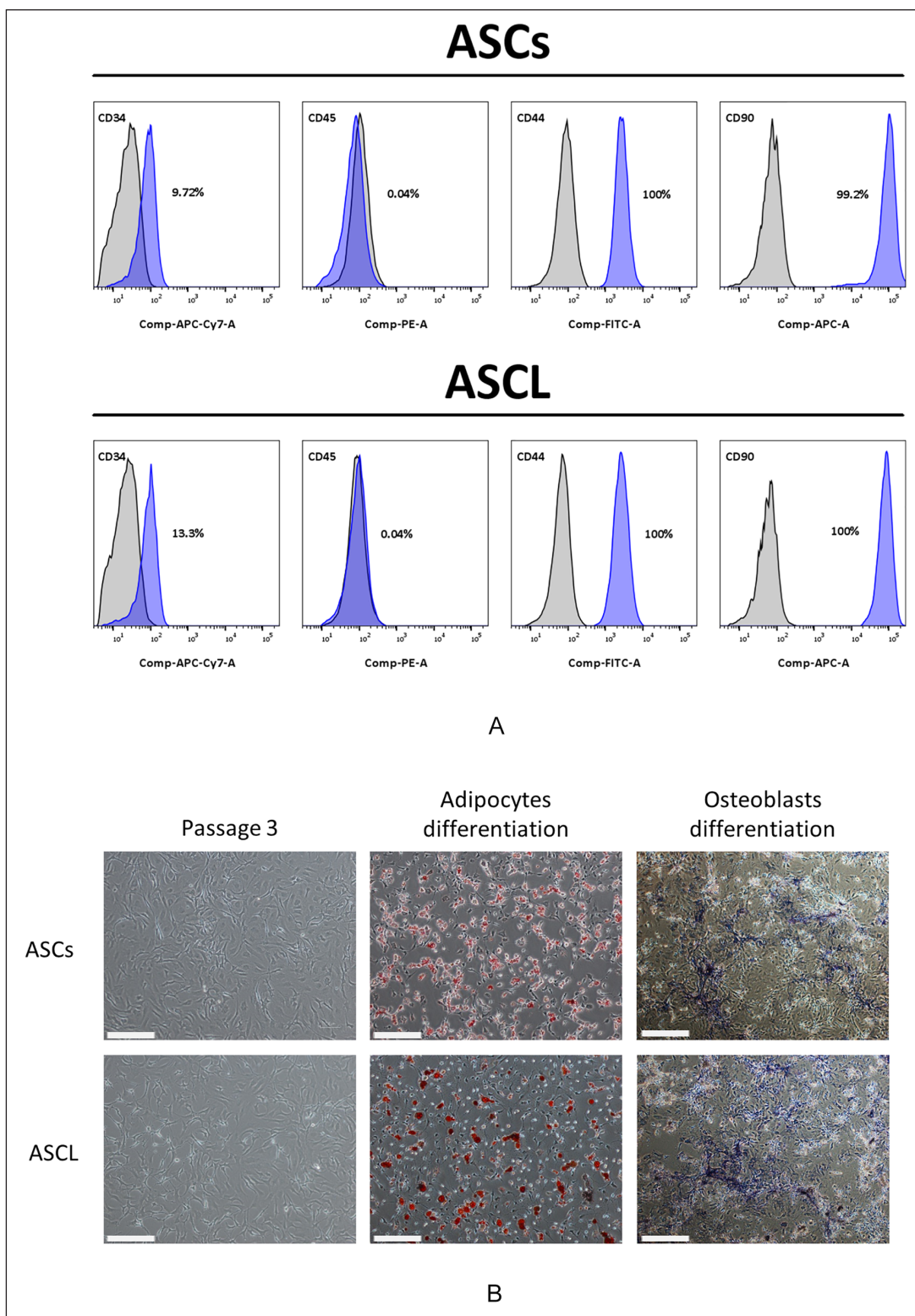


**Figure 1.** Characterization of rat ASCs and ASCL. (A) Immunophenotype of rat ASCs and ASCL. Cells were harvested after the third passage, labeled with antibodies specific for the indicated surface antigen, and analyzed by flow cytometry. The gray zones in the panels represent the negative control and the purple zones represent the population of each surface marker expressed in the cells. The numbers in the panels represent the positive percentage of the expressing markers. (B) Adipocytes and osteoblasts differentiation were induced by rat ASCs and ASCL after third passage. Cells were stained with Oil Red O and alkaline phosphatase. Bar = 100  $\mu$ M. ASCL: adipose-derived mesenchymal stromal/stem cell line; ASCs: adipose-derived MSCs; APC-Cy7: allophycocyanin-Cyanine® 7 conjugates; PE: phycoerythrin; FITC: fluorescein isothiocyanate; APC: allophycocyanin.

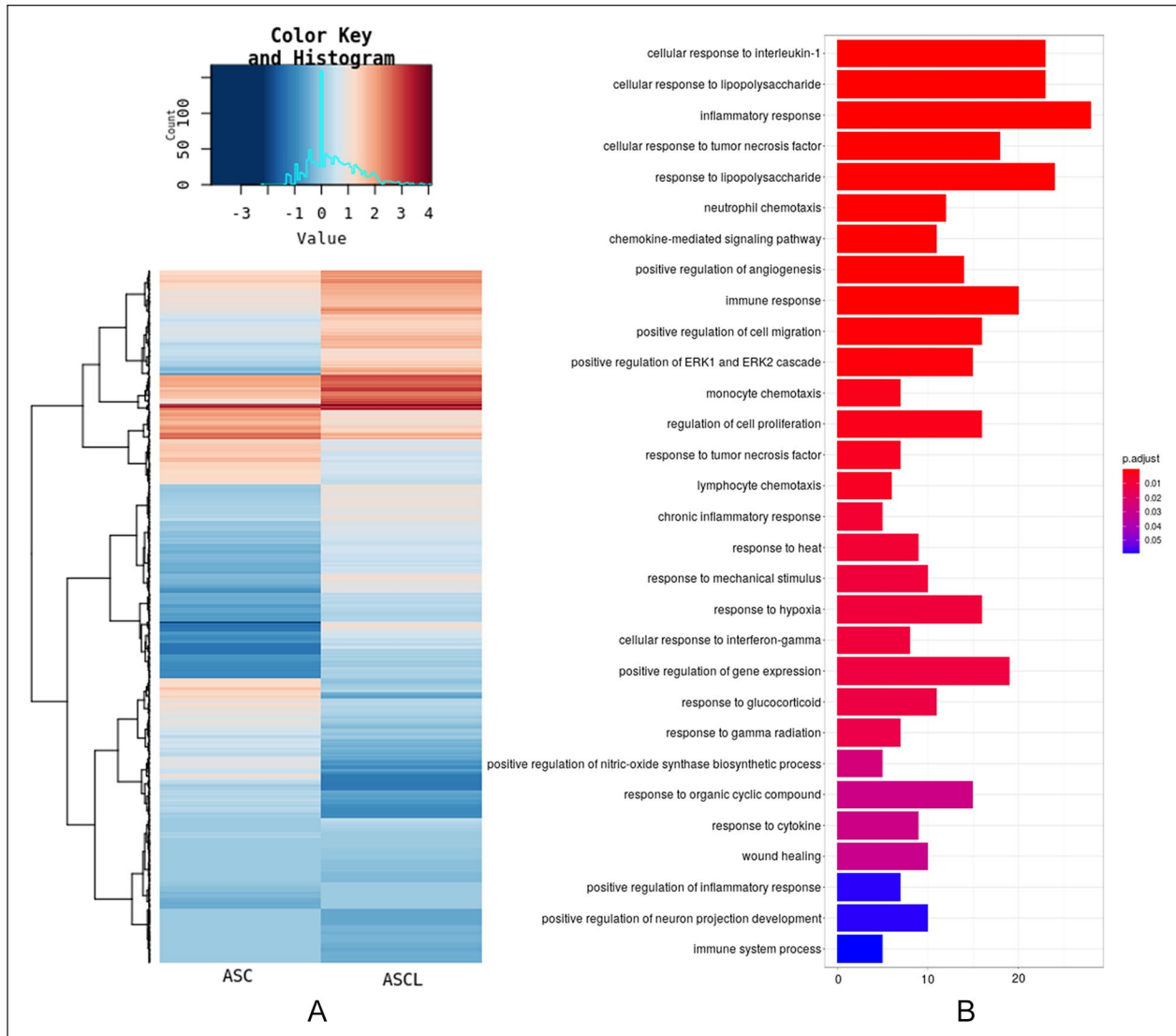


**Figure 2.** RNA-sequencing analysis of rat ASCs and ASCL. RNA was extracted from rat ASCs and ASCL after third passage for sequencing. Differentially expressed genes of ASCL and ASCs (A) were mapped according to the gene ontology database (B). The top 30 upregulated genes in ASCL with lowest false discovery rate ( $FDR \leq 0.05$ ) are presented. ASCL: adipose-derived mesenchymal stromal/stem cell line; ASCs: adipose-derived MSCs.

each group after the hypoxia/reoxygenation treatment. The results showed that TGF- $\beta$  increased in both ASCL ( $P = 0.001$ ) and ASCs ( $P = 0.001$ ) co-culture groups (Fig. 4C), but IL-10 and IL-1Ra only increased in the ASCL co-culture group ( $P = 0.05$  for IL-10 and  $P = 0.009$  for IL-1Ra) (Fig. 4D, E).

### ASCL and ASCs Ameliorated Cell Survival in 120-Min Hepatic IRI

The segmental (70%) warm ischemia in liver sections for 120 min led to a 50% mortality rate in the control group within 10 days. However, the rats pre-infused with ASCL or ASCs successfully survived the hepatic injury during the

observation period and exhibited significant improvement in the survival rate compared with the control group ( $P = 0.048$ ) (Fig. 5).

### ASCL Protects Against 60-Min Hepatic IRI in Decreasing the Liver Enzymes

The serum levels of AST and ALT peaked after 3 h of reperfusion in all three groups. Serum AST and ALT levels were significantly decreased in the ASCL group (AST,  $P = 0.002$ ; ALT,  $P = 0.007$ ); however, no statistical difference was observed in the ASCs group ( $P = 0.302$  in AST,  $P = 0.264$  in ALT) (Fig. 6A) in comparison to the control group after 3 h of reperfusion. All groups entered the recovery stage

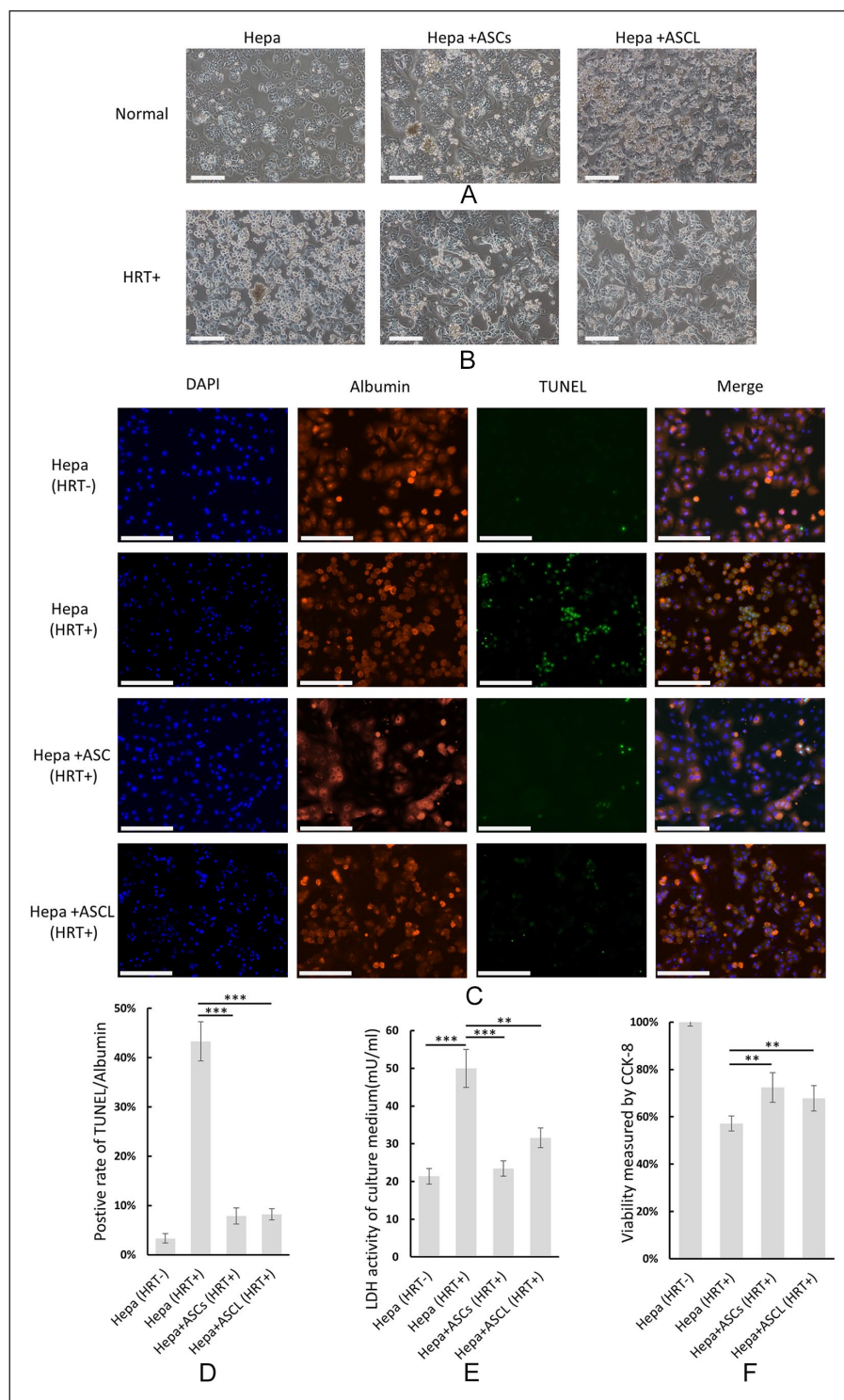


**Figure 3.** ASCs and ASCL attenuate hypoxia/reoxygenation-induced damage to hepatocytes in co-culture. (A) Microscopy images of rat hepatocytes co-cultured with rat ASCs and ASCL; The single culture of rat hepatocytes was the control group. Bar = 100  $\mu$ M. (B) Microscopy images of single culture and co-culture groups after subjected to hypoxia for 3 h followed reoxygenation damage for 1 h. Bar = 100  $\mu$ M. (C) Albumin (Cy5) and TUNEL (GFP) staining of single culture and co-culture groups. Nucleuses were stained with DAPI. Bar = 125  $\mu$ M. (D) TUNEL positive rate of hepatocytes was calculated using the ratio of TUNEL (GFP) to albumin (Cy5). (E) LDH activity in the culture medium of each group post-hypoxia/reoxygenation treatment (n = 3). (F) Evaluation of cell viability of each group using cell counting kit-8 following hypoxia/reoxygenation treatment (n = 3). Data are presented as means  $\pm$  SE. ASCL: adipose-derived mesenchymal stromal/stem cell line; ASCs: adipose-derived MSCs; HRT: hypoxia/reoxygenation treatment; LDH: lactate dehydrogenase; TUNEL: terminal deoxynucleotidyl transferase mediated dUTP nick end labeling; GFP: green fluorescent protein; DAPI: 4',6-diamidino-2-phenylindole. \* $P < 0.05$ . \*\* $P < 0.01$ . \*\*\* $P < 0.001$ .

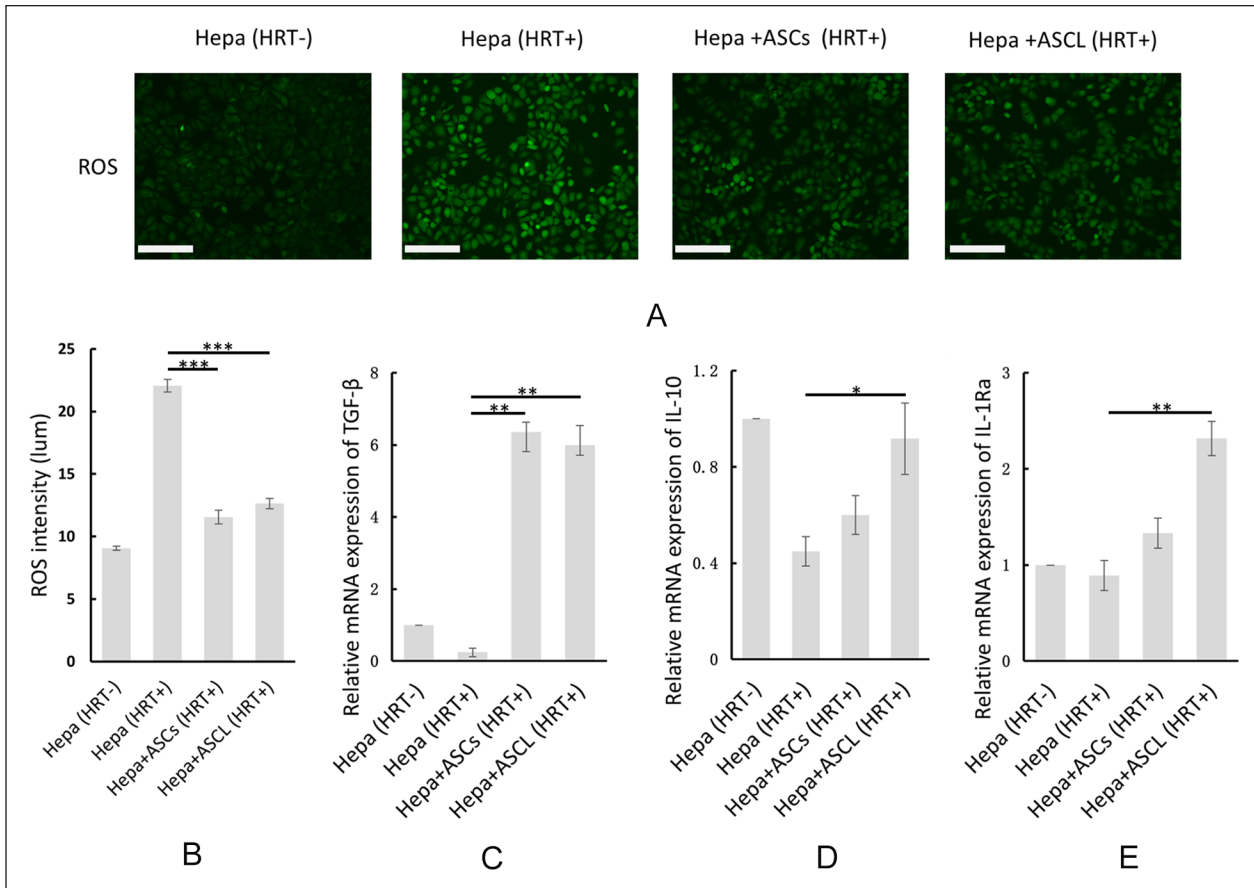


**Figure 4.** ASCL and ASCs protect hepatocytes from ROS damage and alleviate hypoxia/reoxygenation-induced damage by immunoregulation of cytoprotective cytokines. (A and B) ROS intensity in each group following hypoxia/reoxygenation treatment. (C-E) Relative expression of TGF- $\beta$ , IL-10, and IL-1Ra mRNA in hypoxia/reoxygenation-treated hepatocytes compared to the untreated group (sham) ( $n = 3$ ) estimated using qRT-PCR. Data are presented as means  $\pm$  SE. ASCL: adipose-derived mesenchymal stromal/stem cell line; ASCs: adipose-derived MSCs; HRT: hypoxia/reoxygenation treatment; IL: interleukin; qRT-PCR: Quantitative Real-Time Polymerase Chain Reaction; ROS: reactive oxygen species; TGF- $\beta$ : transforming growth factor- $\beta$ . \* $P < 0.05$ . \*\* $P < 0.01$ . \*\*\* $P < 0.001$ .

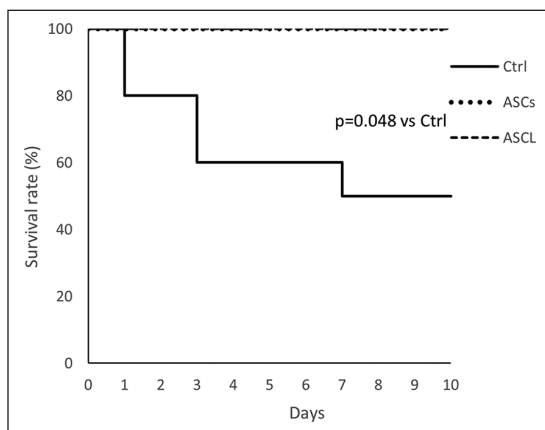


**Figure 5.** ASCL and ASCs enhanced the survival in hepatic IRI for 120 min ( $n = 10$  for control group,  $n = 6$  for ASCL and ASCs group).  $P = 0.048$  in both ASCL and ASCs group compared with the control group. ASCL: adipose-derived mesenchymal stromal/stem cell line; ASCs: adipose-derived MSCs; IRI: ischemia/reperfusion injury.

according to the decrease in serum AST and ALT levels 24 h after reperfusion. The ASCL group showed the most rapid tendency ( $P = 0.130$  in AST,  $P = 0.252$  in ALT), whereas liver enzymes in the control ( $P = 0.013$  in AST,  $P = 0.024$  in ALT) and the ASCs ( $P = 0.006$  in AST,  $P = 0.004$  in ALT) groups showed no change.

### ASCL Prevents Liver Tissue From Lesions and Apoptosis

In the histological study, we evaluated the therapeutic effect by hematoxylin and eosin staining (Fig. 6B) and TUNEL fluorescence staining (Fig. 6C). Lesions occurred early in the peripheral liver lobules after 3 h of reperfusion. After 24 h of reperfusion, severe lesions including cell destruction and vacuolization were spread widely in large areas of liver lobules in the control and ASCs groups, whereas lesions in the ASCL group were limited to small areas of liver lobules. Quantification of the liver damage in each group by the Suzuki score (Fig. 6D) showed a similar tendency, with



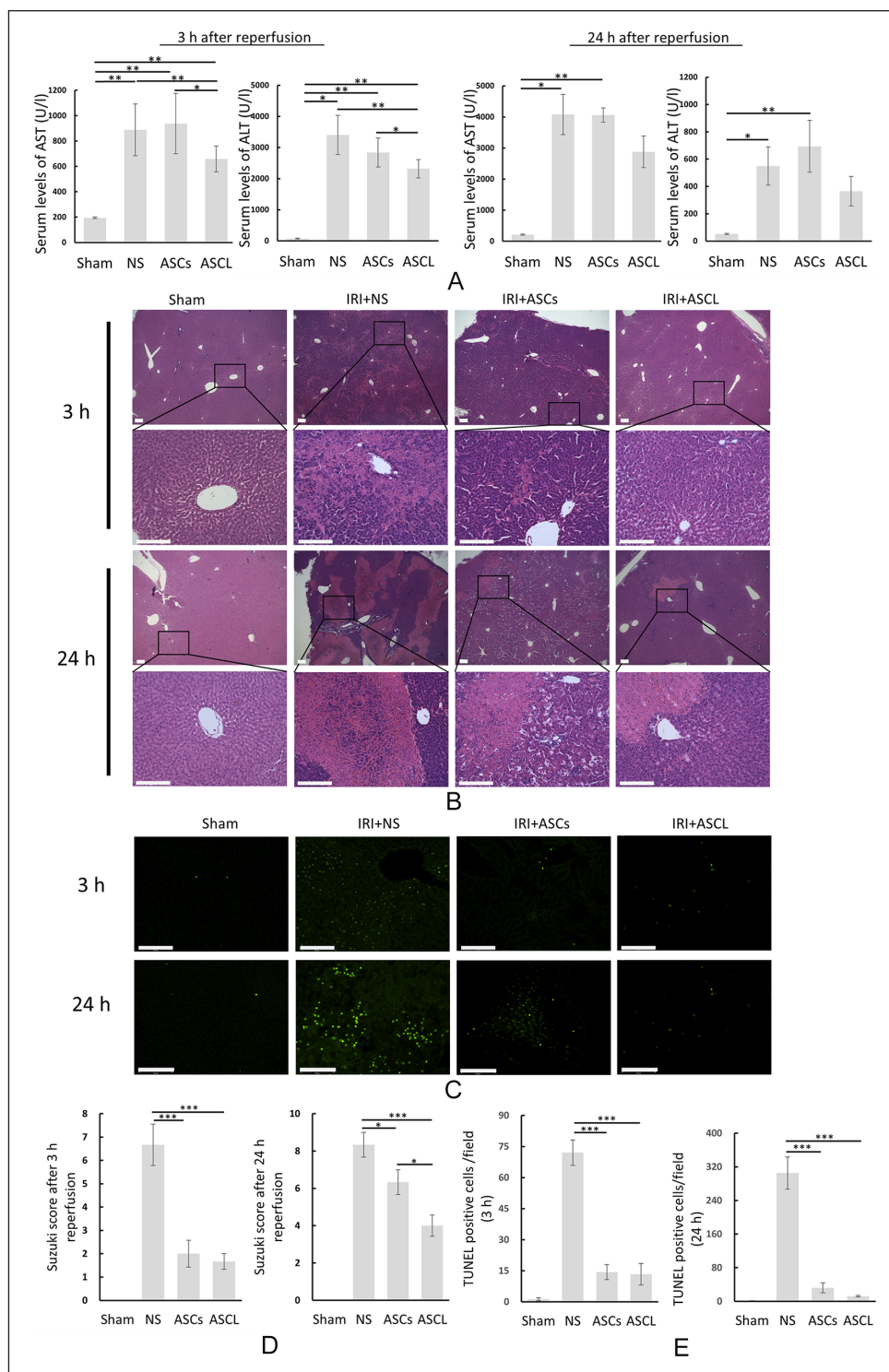


**Figure 6.** ASCL protect against hepatic IRI in vivo. (A) Serum AST and ALT levels were evaluated after 3 and 24 h of hepatic IRI ( $n = 5$ ). (B) Hematoxylin and eosin staining of liver tissues were processed after 3 and 24 h of hepatic IRI in each group (Bar = 125  $\mu$ M). (C) TUNEL staining of injured liver tissues was processed after 3 and 24 h of hepatic IRI in each group (Bar = 125  $\mu$ M). (D) Changes associated with sinusoidal congestion, and hepatocellular vacuolization and necrosis were analyzed based on the Suzuki score. (E) Cell death in liver tissues was calculated by assessing the number of TUNEL (GFP) positive cells per field. Data are presented as means  $\pm$  SE. ALT: alanine aminotransferase; ASCL: adipose-derived mesenchymal stromal/stem cell line; AST: aspartate aminotransferase; IRI: ischemia/reperfusion injury; TUNEL: terminal deoxynucleotidyl transferase mediated dUTP nick end labeling; GFP: green fluorescent protein; NS: normal saline. \* $P < 0.05$ . \*\* $P < 0.01$ . \*\*\* $P < 0.001$ .

scores in the control group being significantly higher than that in the ASCL and ASCs groups after 3 ( $P < 0.001$ ) and 24 h ( $P < 0.001$  in the ASCL group,  $P = 0.034$  in the ASCs group) of reperfusion. Moreover, a statistical difference in the Suzuki score was detected between the ASCL and ASCs groups after 24 h of reperfusion ( $P = 0.018$ ). In the TUNEL assay, positive TUNEL staining was massively detected in the control group at 3 and 24 h of reperfusion, whereas TUNEL expression was impeded in the ASCL ( $P < 0.001$ ) and ASCs ( $P < 0.001$ ) groups (Fig. 6E).

### ASCL and ASC Affect Cytokines Expression During Hepatic IRI

We determined cytokine expression in both liver tissue and serum using qRT-PCR and ELISA, respectively. As shown in Fig. 7A, mRNA expression of IL-1Ra was significantly higher in the ASCL group than in the control ( $P = 0.003$ ) and ASCs ( $P = 0.009$ ) groups. The mRNA expression of IL-6 was significantly higher in the control group than in the ASCL ( $P < 0.001$ ) and ASCs ( $P < 0.001$ ) groups, and the mRNA expression of TGF- $\beta$  and IL-10 increased in the ASCL group compared with that in the control group ( $P = 0.001$  in TGF- $\beta$  and  $P < 0.001$  in IL-10). In the ELISA study (Fig. 7B), we detected a significant increase in serum levels of IL-18 ( $P < 0.001$  vs. ASCL,  $P = 0.017$  vs. ASCs) and IL-6 ( $P < 0.001$ ) but decreased TGF- $\beta$  ( $P = 0.019$  vs. ASCL,  $P = 0.016$  vs. ASCs) in the control group. Serum levels of IL-10 were significantly higher in the ASCL group than in the control group ( $P = 0.042$ ) and ASCs group ( $P = 0.044$ ). IL-1 $\beta$  was nearly undetectable in the serum except for one sample from the control group (132 pg/mL); thus, we alternatively assessed IL-1 $\beta$  expression by western blot analysis.

### ASCL Inhibits NLRP3 Inflammasome and Activates IL-1RA Expression

To further determine the therapeutic effect of ASCL pre-infusion in hepatic IRI, we studied the mechanism underlying the inhibition of rat hepatic IRI pathology by ASCL and ASCs. We tested the protein expression of NLRP3, casp-1, IL-1 $\beta$ , IL-18, and IL-1Ra in IRI liver tissues. As shown in Fig. 7C–E, the relative expressions of NLRP3 and cleaved casp-1 were upregulated in the control group and downregulated in both ASCL ( $P < 0.001$  in NLRP3 and  $P = 0.002$  in casp-1) and ASCs ( $P < 0.001$  in NLRP3 and  $P = 0.003$  in casp-1) groups. The relative expression of IL-1 $\beta$  was downregulated in the ASCL ( $P = 0.003$ ) and ASCs ( $P < 0.001$ ) groups. The relative expression of IL-18 was downregulated in the ASCL ( $P = 0.007$ ) and ASCs ( $P < 0.001$ ) groups. The relative expression of IL-1Ra was upregulated in the ASCL ( $P = 0.027$ ) group, whereas it was significantly downregulated in the ASCs ( $P < 0.001$ ) group.

## Discussion

The present study demonstrated that as ASCs, ASCL has analogous capabilities to protect hepatocytes against *in vitro* hypoxic damage, by prohibiting hepatocyte death, release of ROS, and inducing the gene expression of TGF- $\beta$ . Using *in vivo* rat hepatic IRI model, we established that similar to ASCs, ASCL pre-infusion prevents hepatic IRI by downregulating the expression of the proinflammatory cytokines and inflammasome, along with the inhibition of apoptotic pathway in hepatocytes, and the upregulation of serum TGF- $\beta$ . Moreover, ASCL induced the remarkable upregulation of the anti-inflammatory cytokines, IL-10 and IL-1Ra in both *in vitro* and *in vivo* systems, which were not observed in case of ASCs pre-infusion. Also, ASCL pre-infusion substantially suppressed the serum levels of liver enzymes and alleviated liver tissue damage, indicating a superior survival outcome in lethal hepatic IRI model.

Human ASCs, that is, ASCL, stabilized the induction of megakaryocytes differentiation, as well as that of adipocytes, chondrocytes, and osteoblasts, since the differentiation ability of non-cell-line ASCs varies considerably as a result of its heterogeneity<sup>26</sup>. MSCs-based therapy also poses a similar challenge; we assumed that the characteristics of heterogeneous stromal cells, such as contamination of pericytes, may reduce the effect of MSCs therapy on treatment. Thus, we established a rat ASC line to determine the therapeutic potential of ASCL in hepatic IRI by applying ASCL and ASCs to hepatocytes for *in vitro* hypoxia/recovery treatment and rat hepatic IRI models *in vivo*.

MSCs therapy has recently focused on hepatic IRI. Seki et al.<sup>19</sup> found that ASCs transplantation promotes liver regeneration after hepatic ischemia-reperfusion and subsequent hepatectomy by cytokines and growth factor stimulation, including IL-6, TNF- $\alpha$ , hepatic growth factor, and vascular endothelial growth factor. Li et al.<sup>18</sup> reported that BMMSCs attenuate neutrophil accumulation in hepatic IRI by hindering CXCL2/CXCR2 signaling. Yao et al.<sup>28</sup> also reported that extracellular vesicles (EVs) derived from human umbilical cord MSCs are enriched with manganese superoxide dismutase, which can suppress oxidative stress during hepatic IRI. Several studies have suggested that paracrine properties, instead of bio-distributional differentiation, mainly contribute to the therapeutic effect of MSCs in regenerative medicine<sup>29–31</sup>. MSCs participate in immunoregulation by releasing cytoprotective cytokines and secreting EVs, which eventually inhibit the immune response, suppress apoptosis, and promote the proliferation in injured tissues or organs<sup>11,20,21,28,32</sup>. The present study revealed that ASCL has the similar paracrine function as previously reported MSCs concerning hepatic IRI. Moreover, ASCL can impede NLRP3 activation in hepatic IRI by inhibiting cleavage of casp-1, which eventually hampers the release of IL-1 $\beta$  and IL-18 from their progenitors.

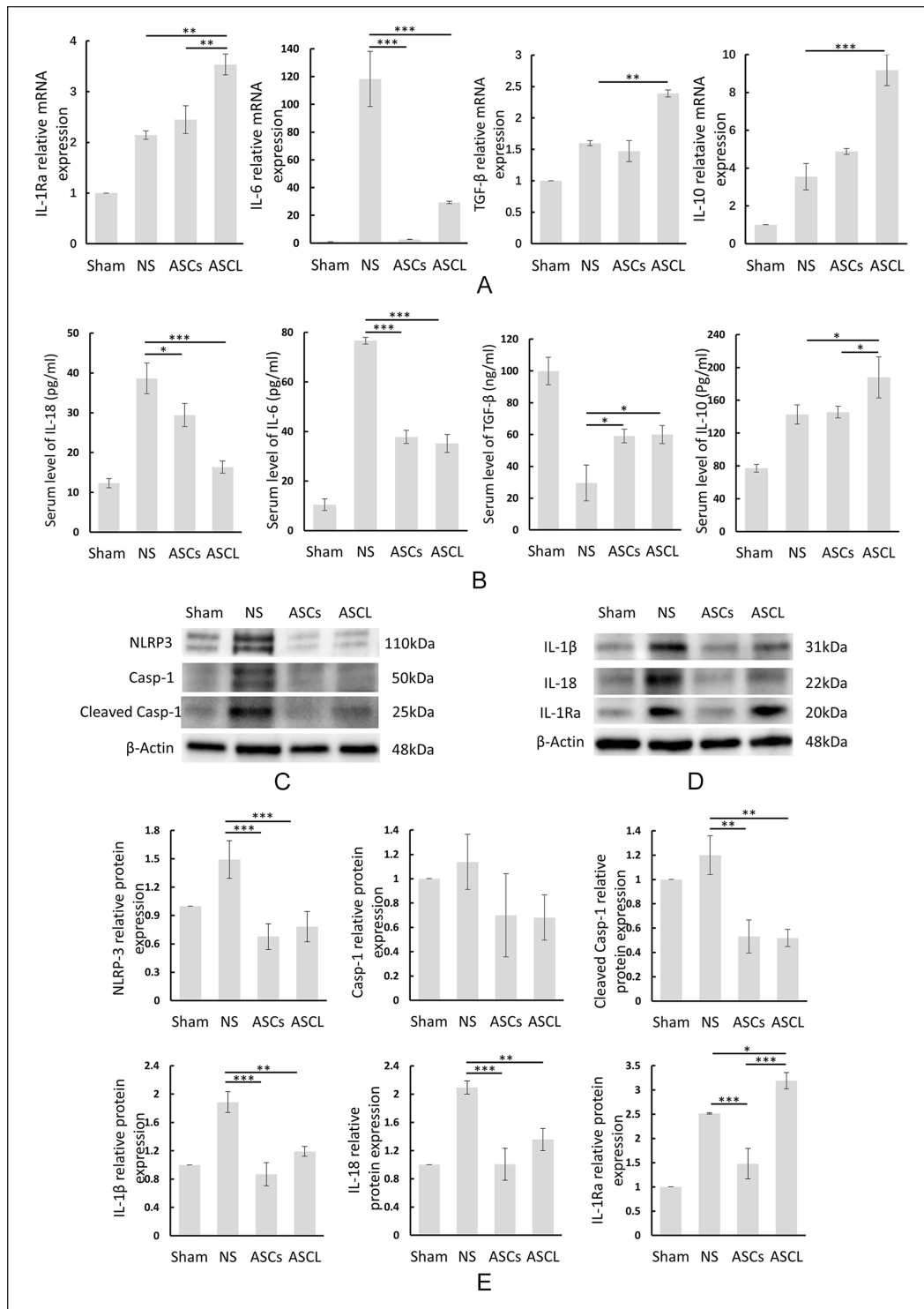


**Figure 7.** ASCL protect against hepatic IRI in vivo by inhibiting NLRP3 inflammasome and activating IL-1RA expression. (A) Relative expression of IL-1Ra, IL-6, TGF-β, and IL-10 mRNA in each hepatic IRI lobe were evaluated using qRT-PCR (n = 3). (B) Serum levels of IL-18, IL-6, TGF-β, and IL-10 were measured using ELISA (n = 4–5). ASCL (C, D) Relative protein expression of NLRP-3-related proteins from liver tissues of each group of hepatic IRI was estimated using western blot analysis. (E) The average band intensities in the western blots were quantified relative to those of the sham group using β-actin as an internal reference (n = 3). Data are presented as means ± SE. ASCL: adipose-derived mesenchymal stromal/stem cell line; ASCs: adipose-derived MSCs; ELISA: enzyme-linked immunosorbent assay; IL: interleukin; IRI: ischemia/reperfusion injury; NLRP-3: NOD-like receptor family pyrin domain-containing 3; qRT-PCR: quantitative real-time polymerase chain reaction; TGF-β: transforming growth factor-β; NS: normal saline. \**P* < 0.05. \*\**P* < 0.01. \*\*\**P* < 0.001.

NLRP3 inflammasome activation is an essential pathogenic mechanism underlying all types of liver diseases<sup>33–35</sup>. In the case of hepatic IRI, release of pathogen-related molecular patterns and danger-associated molecular patterns, derived from damaged hepatocytes, liver sinusoidal endothelial cells, and recruits of Kupffer cells, including cholesterol crystals, palmitic acid, DNA fragments, and ROS, trigger the complement of NLRP3 inflammasome to initiate the activation of pro-casp-1, entailing the downstream cleavage of IL-1 $\beta$  and IL-18 into mature forms. Secretion of these cytokines further leads to the accumulation of neutrophils and macrophages to induce inflammation of damaged liver tissue. In addition, secretion of IL-1 $\beta$  may interact with and activate IL-1 receptor to amplify the inflammatory signal, which eventually causes liver tissue undergoing NLRP3 inflammasome-related programmed cell death known as pyroptosis<sup>35</sup>.

In addition, IL-1Ra, another key factor in the regeneration of inflammatory diseases<sup>36–41</sup>, was found to be highly expressed in ASCL group. We previously reported that IL-1Ra gene delivery into the liver can protect rats against hepatic IRI<sup>42</sup>. Other studies have reported that IL-1Ra over-expressed MSCs can reduce nuclear factor kappa B expression triggered by activation of IL-1R to decrease IL-1, TNF- $\alpha$ , and IL-6 from Kupffer cells, which substantially attenuates liver damage in terms of inflammatory responses and reduces mortality rates<sup>36,38,41</sup>. Although ASCs can hardly modulate the expression of IL-1Ra without any modification<sup>36,37</sup>, significantly increased expression of IL-1Ra can be observed in the unmodified ASCL. GO analysis using RNA-sequencing also strengthened the evidence that ASCL is more sensitive to hypoxia response and inflammatory response, especially in IL-1-related inflammatory response. Therefore, ASCL has more stabilized outcomes in hepatic IRI treatment than ASCs.

In a preliminary study, we injected ASCL/ASCs intravenously immediately after lethal rat hepatic IRI induction. The 10-day survival rates showed no significant difference between the control group and ASCL or ASC groups (Supplemental Fig. 1). In addition, incisional hematoma and nasal bleeding occurred in the ASCL and ASC groups after hepatic IRI induction. It has been reported that intravenous stem cell therapy can result in pulmonary embolism and lead to death<sup>43–45</sup>, especially because intravenous injection of cells may further deteriorate hemodynamics, already affected by the previous blood supply occlusion in the portal vein and hepatic artery. To minimize the side effects of ASCL/ASCs infusion, we used intrasplenic injection 24 h before hepatic IRI induction. We estimated that pre-infusion with ASCL/ASCs had the least influence on hemodynamics as most intrasplenic infused MSCs will enter the liver sinusoids, and eventually migrate in the liver parenchyma<sup>45</sup>. Furthermore, as hepatic IRI is characterized by rapid Kupffer cell activation soon after reperfusion<sup>2,4</sup>, a 24-h pre-infusion can help

migrated ASCL/ASCs in injury response. Previously, we demonstrated that suppression of the inflammatory response may prolong graft survival and improve liver function early after transplantation<sup>46,47</sup>. We expected that this treating strategy described in the present study can serve as basis for new approaches in clinical practice for a preventive treatment in the perioperative period of liver transplantation. However, further experiments are required to confirm whether ASCL has the same *in vivo* distribution as the previously reported MSCs infused via spleen. Moreover, whether the immunomodulation of NLRP3 inflammasome and IL-1Ra as we described in this study or other functional processes such as direct interaction with the liver by intraportal migration are the principal therapeutic effects of ASCL ameliorating hepatic IRI remains elusive due to the intricate underlying molecular mechanism of the hepatic IRI process. In addition, recent reports have focused on MSCs-derived exosome therapy to circumvent the limitations caused by the side effects of direct cell injection or transplantation. Moreover, this cell-free therapy has been confirmed to have a variety of beneficial effects in regenerative diseases, including liver diseases<sup>28,48–51</sup>. Thus, application of ASCL or other cell line MSCs in exosome-based therapy may emerge as a novel and improved concept for regenerative medicine in future research. Although MSCs exosome-based therapy has achieved significant progress in recent years, exosomes isolated from MSCs also inherit their heterogeneity, which hinders the consistency in their treatment<sup>48,50</sup>. We believe that further studies on ASCL-based exosome therapy deserve to be pursued and further explored as it might be a promising therapeutic solution.

In conclusion, our findings demonstrated the therapeutic potential of ASCL in effectively treating hepatic IRI by impeding the activation of NLRP3 inflammasome and release of IL-1Ra, thereby protecting injured liver tissue from pyroptosis and apoptosis. Considering ASCL as a stable cell line of ASCs, the results of the present study may provide a novel and effective strategy for liver transplantation or hepatic IRI treatment in clinical practice.

### Acknowledgments

The authors thank Kazuhiro Miyao and Michiru Sugimoto for their technical assistance.

### Author Contribution

Kaili Chen, Kazumasa Fukuda, and Hideaki Obara acquired and analyzed the data. Yumiko Matsubara and Yukako Ono-Uruga established and provided rat adipose-derived mesenchymal stromal/stem cell line. Kaili Chen, Kazumasa Fukuda, Kentaro Matsubara, Hiroshi Yagi, and Hideaki Obara were involved in study design and drafting the manuscript. Hideaki Obara and Yuko Kitagawa contributed to editing and reviewing. Hideaki Obara, Yukako Ono-Uruga, and Yumiko Matsubara obtained the funding. All authors critically revised the report, commented on drafts of the manuscript, and approved the final report.



## Ethical Approval

This study was approved by the Ethics Committee of Keio University (Approval Number: 20018).

## Statement of Human and Animal Rights

All experimental procedures involving animals were conducted in accordance with the animal experiment guidelines issued by the Laboratory Animal Center, Keio University School of Medicine (Approval Number: 20018).

## Statement of Informed Consent

There are no human subjects in this article and informed consent is not applicable.

## Declaration of Conflicting Interest

The author(s) declared the following potential conflicts of interest with respect to the research, authorship, and/or publication of this article: Yukako Ono-Uruga and Yumiko Matsubara hold shares in AdipoSeeds, Inc. Dr Kitagawa reports grants from CHUGAI PHARMACEUTICAL CO., LTD., grants from TAIHO PHARMACEUTICAL CO., LTD, grants from Yakult Honsha Co. Ltd., grants from ASAHI KASEI PHARMA CORPORATION, grants from Otsuka Pharmaceutical Co., Ltd., grants from Takeda Pharmaceutical Co., Ltd., grants from ONO PHARMACEUTICAL CO., LTD., grants from TSUMURA & CO., grants from Kyouwa Hakkou Kirin Co., Ltd., grants from EA Pharma Co., Ltd., grants from MEDICON INC., grants from KAKEN PHARMACEUTICAL CO. LTD., grants from Eisai Co., Ltd., grants from Otsuka Pharmaceutical Factory Inc., grants from TEIJIN PHARMA LIMITED., grants from NIHON PHARMACEUTICAL CO., LTD., grants from Nippon Covidien Inc., personal fees from ASAHI KASEI PHARMA CORPORATION, personal fees from AstraZeneca K.K., personal fees from Ethicon Inc., personal fees from ONO PHARMACEUTICAL CO., LTD., personal fees from Otsuka Pharmaceutical Factory, Inc., personal fees from Olympus Corporation, personal fees from Nippon Covidien Inc., personal fees from SHIONOGI & CO., LTD., personal fees from TAIHO PHARMACEUTICAL CO., LTD, personal fees from CHUGAI PHARMACEUTICAL CO., LTD., personal fees from Bristol-Myers Squibb K.K., personal fees from MSD K.K., personal fees from Smith & Nephew KK, personal fees from KAKEN PHARMACEUTICAL CO.,LTD., and personal fees from ASKA Pharmaceutical Co., Ltd. outside the submitted work.

## Funding

The author(s) disclosed receipt of the following financial support for the research, authorship, and/or publication of this article: Hideaki Obara receives research support from Grant-in-Aid for Scientific Research (C) 20K09087. Yukako Ono-Uruga and Yumiko Matsubara receive research support from AdipoSeeds, Inc.

## ORCID iD

Hideaki Obara  <https://orcid.org/0000-0001-6740-2715>

## Supplemental Material

Supplemental material for this article is available online.

## References

1. Elias-Miro M, Jimenez-Castro MB, Rodes J, Peralta C. Current knowledge on oxidative stress in hepatic ischemia/reperfusion. *Free Radic Res.* 2013;47(8):555–68.
2. Konishi T, Lentsch AB. Hepatic ischemia/reperfusion: mechanisms of tissue injury, repair, and regeneration. *Gene Expr.* 2017;17(4):277–87.
3. Selzner N, Selzner M, Jochum W, Clavien P-A. Ischemic preconditioning protects the steatotic mouse liver against reperfusion injury: an ATP dependent mechanism. *J Hepatol.* 2003;39(1):55–61.
4. Teoh NC, Farrell GC. Hepatic ischemia reperfusion injury: pathogenic mechanisms and basis for hepatoprotection. *J Gastroenterol Hepatol.* 2003;18:891–902.
5. Zhang Q, Piao C, Xu J, Jiao Z, Ge Y, Liu X, Ma Y, Wang H. Comparative study on protective effect of hydrogen rich saline and adipose-derived stem cells on hepatic ischemia-reperfusion and hepatectomy injury in swine. *Biomed Pharmacother.* 2019;120:109453.
6. Pittenger MF, Mackay AM, Beck SC, Jaiswal RK, Douglas R, Mosca JD, Moorman MA, Simonetti DW, Craig S, Marshak DR. Multilineage potential of adult human mesenchymal stem cells. *Science.* 1999;284(5411):143–47.
7. Ding DC, Chang YH, Shyu WC, Lin SZ. Human umbilical cord mesenchymal stem cells: a new era for stem cell therapy. *Cell Transplant.* 2015;24(3):339–47.
8. Forbes SJ, Gupta S, Dhawan A. Cell therapy for liver disease: from liver transplantation to cell factory. *J Hepatol.* 2015; 62(Suppl 1): S157–69.
9. Galipeau J, Sensebe L. Mesenchymal stromal cells: clinical challenges and therapeutic opportunities. *Cell Stem Cell.* 2018; 22(6):824–33.
10. Li N, Hua J. Interactions between mesenchymal stem cells and the immune system. *Cell Mol Life Sci.* 2017;74(13):2345–60.
11. Wang YH, Wu DB, Chen B, Chen EQ, Tang H. Progress in mesenchymal stem cell-based therapy for acute liver failure. *Stem Cell Res Ther.* 2018;9(1):227.
12. Vosough M, Moslem M, Pournasr B, Baharvand H. Cell-based therapeutics for liver disorders. *Br Med Bull.* 2011;100: 157–72.
13. Lo Nigro A, Gallo A, Bulati M, Vitale G, Pains DS, Pampalone M, Galvagno D, Conaldi PG, Miceli V. Amnion-derived mesenchymal stromal/stem cell paracrine signals potentiate human liver organoid differentiation: translational implications for liver regeneration. *Front Med (Lausanne).* 2021;8:746298.
14. de Miguel MP, Prieto I, Moratilla A, Arias J, Aller MA. Mesenchymal stem cells for liver regeneration in liver failure: from experimental models to clinical trials. *Stem Cells Int.* 2019;2019:3945672.
15. Hu C, Wu Z, Li L. Pre-treatments enhance the therapeutic effects of mesenchymal stem cells in liver diseases. *J Cell Mol Med.* 2020;24(1):40–49.
16. Isbambetov A, Baimakhanov Z, Soyama A, Hidaka M, Sakai Y, Takatsuki M, Kuroki T, Eguchi S. Equal distribution of mesenchymal stem cells after hepatic ischemia-reperfusion injury. *J Surg Res.* 2016;203(2):360–67.
17. Jiao Z, Liu X, Ma Y, Ge Y, Zhang Q, Liu B, Wang H. Adipose-derived stem cells protect ischemia-reperfusion and partial hepatectomy by attenuating endoplasmic reticulum stress. *Front Cell Dev Biol.* 2020;8:177.

18. Li S, Zheng X, Li H, Zheng J, Chen X, Liu W, Tai Y, Zhang Y, Wang G, Yang Y. Mesenchymal stem cells ameliorate hepatic ischemia/reperfusion injury via inhibition of neutrophil recruitment. *J Immunol Res.* 2018;2018:7283703.
19. Seki T, Yokoyama Y, Nagasaki H, Kokuryo T, Nagino M. Adipose tissue-derived mesenchymal stem cell transplantation promotes hepatic regeneration after hepatic ischemia-reperfusion and subsequent hepatectomy in rats. *J Surg Res.* 2012;178(1):63–70.
20. Liang X, Ding Y, Zhang Y, Tse HF, Lian Q. Paracrine mechanisms of mesenchymal stem cell-based therapy: current status and perspectives. *Cell Transplant.* 2014;23(9):1045–59.
21. Miceli V, Bulati M, Iannolo G, Zito G, Gallo A, Conaldi PG. Therapeutic properties of mesenchymal stromal/stem cells: the need of cell priming for cell-free therapies in regenerative medicine. *Int J Mol Sci.* 2021;22(2):763.
22. Detry O, Vandermeulen M, Delbouille MH, Somja J, Bletard N, Briquet A, Lechanteur C, Giet O, Baudoux E, Hannon M, Baron F, et al. Infusion of mesenchymal stromal cells after deceased liver transplantation: a phase I-II, open-label, clinical study. *J Hepatol.* 2017;67(1):47–55.
23. Mohamadnejad M, Alimoghaddam K, Bagheri M, Ashrafi M, Abdollahzadeh L, Akhlaghpour S, Bashtar M, Ghavamzadeh A, Malekzadeh R. Randomized placebo-controlled trial of mesenchymal stem cell transplantation in decompensated cirrhosis. *Liver Int.* 2013;33(10):1490–96.
24. Peng L, Xie DY, Lin BL, Liu J, Zhu HP, Xie C, Zheng YB, Gao ZL. Autologous bone marrow mesenchymal stem cell transplantation in liver failure patients caused by hepatitis B: short-term and long-term outcomes. *Hepatology.* 2011;54(3):820–28.
25. Suk KT, Yoon JH, Kim MY, Kim CW, Kim JK, Park H, Hwang SG, Kim DJ, Lee BS, Lee SH, Kim HS, et al. Transplantation with autologous bone marrow-derived mesenchymal stem cells for alcoholic cirrhosis: phase 2 trial. *Hepatology.* 2016;64(6):2185–97.
26. Tozawa K, Ono-Uruga Y, Yazawa M, Mori T, Murata M, Okamoto S, Ikeda Y, Matsubara Y. Megakaryocytes and platelets from a novel human adipose tissue-derived mesenchymal stem cell line. *Blood.* 2019;133(7):633–43.
27. Fujii T, Obara H, Matsubara K, Fujimura N, Yagi H, Hibi T, Abe Y, Kitago M, Shinoda M, Itano O, Tanabe M, et al. Oral administration of cilostazol improves survival rate after rat liver ischemia/reperfusion injury. *J Surg Res.* 2017;213:207–14.
28. Yao J, Zheng J, Cai J, Zeng K, Zhou C, Zhang J, Li S, Li H, Chen L, He L, Chen H, et al. Extracellular vesicles derived from human umbilical cord mesenchymal stem cells alleviate rat hepatic ischemia-reperfusion injury by suppressing oxidative stress and neutrophil inflammatory response. *FASEB J.* 2019;33(2):1695–1710.
29. Wang H, Zhao T, Xu F, Li Y, Wu M, Zhu D, Cong X, Liu Y. How important is differentiation in the therapeutic effect of mesenchymal stromal cells in liver disease. *Cytotherapy.* 2014;16(3):309–18.
30. Zagoura DS, Roubelakis MG, Bitsika V, Trohatou O, Pappa KI, Kapelouzou A, Antsaklis A, Anagnostou NP. Therapeutic potential of a distinct population of human amniotic fluid mesenchymal stem cells and their secreted molecules in mice with acute hepatic failure. *Gut.* 2012;61(6):894–906.
31. Chen X, Armstrong MA, Li G. Mesenchymal stem cells in immunoregulation. *Immunol Cell Biol.* 2006;84(5):413–21.
32. Maacha S, Sidahmed H, Jacob S, Gentilcore G, Calzone R, Grivel JC, Cugno C. Paracrine mechanisms of mesenchymal stromal cells in angiogenesis. *Stem Cells Int.* 2020;2020:4356359.
33. Witek RP, Stone WC, Karaca FG, Syn WK, Pereira TA, Agboola KM, Omenetti A, Jung Y, Teaberry V, Choi SS, Guy CD, et al. Pan-caspase inhibitor VX-166 reduces fibrosis in an animal model of nonalcoholic steatohepatitis. *Hepatology.* 2009;50(5):1421–30.
34. Wree A, Eguchi A, McGeough MD, Pena CA, Johnson CD, Canbay A, Hoffman HM, Feldstein AE. NLRP3 inflammasome activation results in hepatocyte pyroptosis, liver inflammation, and fibrosis in mice. *Hepatology.* 2014;59(3):898–910.
35. Al Mamun A, Akter A, Hossain S, Sarker T, Safa SA, Mustafa QG, Muhammad SA, Munir F. Role of NLRP3 inflammasome in liver disease. *J Dig Dis.* 2020;21(8):430–36.
36. Xiao JQ, Shi XL, Ma HC, Tan JJ, Lin z Xu Q, Ding YT. Administration of IL-1Ra chitosan nanoparticles enhances the therapeutic efficacy of mesenchymal stem cell transplantation in acute liver failure. *Arch Med Res.* 2013;44(5):370–79.
37. Sang JF, Shi XL, Han B, Huang X, Huang T, Ren HZ, Ding YT. Combined mesenchymal stem cell transplantation and interleukin-1 receptor antagonism after partial hepatectomy. *World J Gastroenterol.* 2016;22(16):4120–35.
38. Gehrke N, Hovelmeyer N, Waisman A, Straub BK, Weinmann-Menke J, Worns MA, Galle PR, Schattenberg JM. Hepatocyte-specific deletion of IL-1-RI attenuates liver injury by blocking IL-1 driven autoinflammation. *J Hepatol.* 2018;68(5):986–95.
39. Petrasek J, Bala S, Csak T, Lippai D, Kodys K, Menashy V, Barrieau M, Min SY, Kurt-Jones EA, Szabo G. IL-1 receptor antagonist ameliorates inflammasome-dependent alcoholic steatohepatitis in mice. *J Clin Invest.* 2012;122(10):3476–89.
40. Meier RPH, Meyer J, Montanari E, Lacotte S, Balaphas A, Muller YD, Clement S, Negro F, Toso C, Morel P, Buhler L. Interleukin-1 receptor antagonist modulates liver inflammation and fibrosis in mice in a model-dependent manner. *Int J Mol Sci.* 2019;20(6):1295.
41. Harrell CR, Markovic BS, Fellabaum C, Arsenijevic N, Djonov V, Volarevic V. The role of Interleukin 1 receptor antagonist in mesenchymal stem cell-based tissue repair and regeneration. *Biofactors.* 2020;46(2):263–75.
42. Harada H, Wakabayashi G, Takayanagi A, Shimazu M, Matsumoto K, Obara H, Shimizu N, Kitajima M. Transfer of the interleukin-1 receptor antagonist gene into rat liver abrogates hepatic ischemia-reperfusion injury. *Transplantation.* 2002;74(10):1434–41.
43. Jung JW, Kwon M, Choi JC, Shin JW, Park IW, Choi BW, Kim JY. Familial occurrence of pulmonary embolism after intravenous, adipose tissue-derived stem cell therapy. *Yonsei Med J.* 2013;54(5):1293–96.
44. Takahashi Y, Tsuji O, Kumagai G, Hara CM, Okano HJ, Miyawaki A, Toyama Y, Okano H, Nakamura M. Comparative study of methods for administering neural stem/progenitor cells to treat spinal cord injury in mice. *Cell Transplant.* 2011;20(5):727–39.

45. Ju S, Teng GJ, Lu H, Zhang Y, Zhang A, Chen F, Ni Y. In vivo MR tracking of mesenchymal stem cells in rat liver after intrasplenic transplantation. *Radiology*. 2007;245(1):206–15.
46. Obara H, Nagasaki K, Hsieh CL, Ogura Y, Esquivel CO, Martinez OM, Krams SM. IFN-gamma, produced by NK cells that infiltrate liver allografts early after transplantation, links the innate and adaptive immune responses. *Am J Transplant*. 2005;5(9):2094–2103.
47. Ono S, Obara H, Takayanagi A, Tanabe M, Kawachi S, Itano O, Shinoda M, Kitago M, Hibi T, Chiba T, Du W, et al. Suppressive effects of interleukin-18 on liver function in rat liver allografts. *J Surg Res*. 2012;176(1):293–300.
48. Roccaro AM, Sacco A, Maiso P, Azab AK, Tai YT, Reagan M, Azab F, Flores LM, Campigotto F, Weller E, Anderson KC, et al. BM mesenchymal stromal cell-derived exosomes facilitate multiple myeloma progression. *J Clin Invest*. 2013;123(4):1542–55.
49. Sun Y, Shi H, Yin S, Ji C, Zhang X, Zhang B, Wu P, Shi Y, Mao F, Yan Y, Xu W, et al. Human mesenchymal stem cell derived exosomes alleviate type 2 diabetes mellitus by reversing peripheral insulin resistance and relieving beta-cell destruction. *ACS Nano*. 2018;12(8):7613–28.
50. Bliss SA, Sinha G, Sandiford OA, Williams LM, Engelberth DJ, Guiro K, Isenalumhe LL, Greco SJ, Ayer S, Bryan M, Kumar R, et al. Mesenchymal stem cell-derived exosomes stimulate cycling quiescence and early breast cancer dormancy in bone marrow. *Cancer Res*. 2016;76(19):5832–44.
51. van Poll D, Parekkadan B, Cho CH, Berthiaume F, Nahmias Y, Tilles AW, Yarmush ML. Mesenchymal stem cell-derived molecules directly modulate hepatocellular death and regeneration in vitro and in vivo. *Hepatology*. 2008;47(5):1634–43.